

# Learning Co-Speech Gesture for Multimodal Aphasia Type Detection

Daeun Lee<sup>1\*</sup>, Sejung Son<sup>1\*</sup>, Hyolim Jeon<sup>1,2</sup>, Seungbae Kim<sup>3</sup>, Jinyoung Han<sup>1,2†</sup>

<sup>1</sup>Department of Applied Artificial Intelligence, Sungkyunkwan University, Seoul, South Korea

<sup>2</sup>Department of Human-AI Interaction, Sungkyunkwan University, Seoul, South Korea

<sup>3</sup>Department of Computer Science & Engineering, University of South Florida, Tampa, FL, USA

{delee12, jinyoungan}@skku.edu

{maze0717, gyfla1512}@g.skku.edu, seungbae@usf.edu

## Abstract

Aphasia, a language disorder resulting from brain damage, requires accurate identification of specific aphasia types, such as Broca’s and Wernicke’s aphasia, for effective treatment. However, little attention has been paid to developing methods to detect different types of aphasia. Recognizing the importance of analyzing co-speech gestures for distinguish aphasia types, we propose a multimodal graph neural network for aphasia type detection using speech and corresponding gesture patterns. By learning the correlation between the speech and gesture modalities for each aphasia type, our model can generate textual representations sensitive to gesture information, leading to accurate aphasia type detection. Extensive experiments demonstrate the superiority of our approach over existing methods, achieving state-of-the-art results (F1 84.2%). We also show that gesture features outperform acoustic features, highlighting the significance of gesture expression in detecting aphasia types. We provide the codes for reproducibility purposes<sup>1</sup>.

## 1 Introduction

*Aphasia* is a language disorder caused by brain structure damage affecting speech functions, commonly triggered by stroke and other factors such as brain injury, dementia, and mental disorder (Broca et al., 1861; Wasay et al., 2014). Depending on prominent symptoms and severity, aphasia can be classified into the eight types (Kertesz, 2007) such as Broca’s and Wernicke’s aphasia as shown in Figure 5 in Appendix. People with aphasia (PWA) can face various communication challenges due to limited language processing and comprehension capabilities, which can result in difficulties with social interaction (El Hachioui et al., 2017). Since

\*Equal contribution.

†Corresponding author.

<sup>1</sup>Code: [https://github.com/DSAIL-SKKU/Multimodal-Aphasia-Type-Detection\\_EMNLP\\_2023](https://github.com/DSAIL-SKKU/Multimodal-Aphasia-Type-Detection_EMNLP_2023)

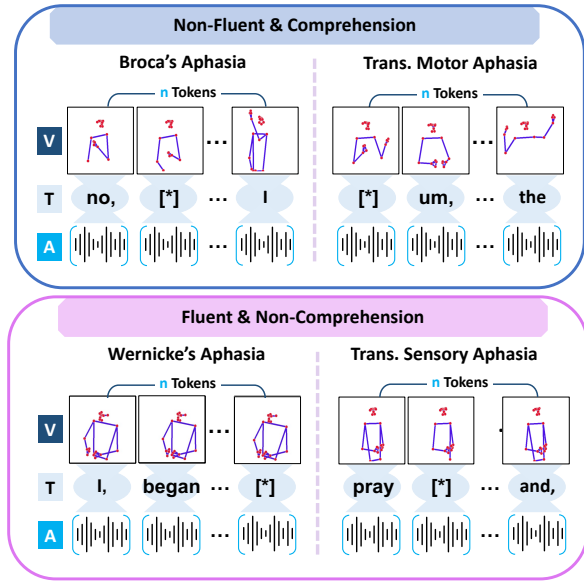


Figure 1: Variations in gestures observed across different types of aphasia. Each aligned data (text, audio, gesture) is extracted using Automatic Speech Recognition (ASR) (§3).

the traditional assessments for PWA are known to be time-consuming and costly (Wilson et al., 2018), identifying the pathological language impairment from speech data has received great attention (Qin et al., 2018a; Fraser et al., 2014). Clinically, a detailed diagnosis of aphasia type is imperative for proper treatment procedures; however, little attention has been paid to developing a classification model for the types of aphasia.

For diagnosing various types of aphasia, analyzing the co-speech gestures of PWA can be essential. PWA often rely on non-verbal communication techniques, especially gestures, as an additional communication tool due to difficulties in word retrieval and language errors (Preisig et al., 2018; de Kleine et al., 2023). Therefore, the same word can be interpreted differently depending on the accompanying gestures for different aphasia types. For example, as shown in Figure 1, individuals with Broca’s aphasia show a higher frequency of iconic

gestures because Broca’s area damage results in preserving semantic content but being impaired fluency (Albert et al., 1973). On the other hand, individuals with Wernicke’s aphasia tend to derive limited assistance from gestures since fluent but incoherent speech pathology (Helm-Estabrooks, 2002). Hence, since the meaning of the word ‘I’ from PWA with Broca’s aphasia may have more latent information, utilizing both speech (i.e., linguistic and acoustic) and gesture (i.e., visual) information is crucial in classifying aphasia types.

In combining two different modalities, speech and gesture, applying the existing multimodal fusion models is challenging due to the following two limitations. First, the existing models were usually built upon emotion recognition or sentiment analysis benchmarks (Zadeh et al., 2016; Busso et al., 2008) mainly consisting of facial information; yet, PWA struggles in using faces caused by the impaired emotion processing (Multani et al., 2017). Second, these models tended to capture a single link across the modalities, e.g., linking happiness-related words to smiling faces (Yang et al., 2021; Tsai et al., 2019), but there can be multiple links across the modalities depending on aphasia types. (e.g., ‘I’ may be connected to multiple gestures based on aphasia types, as shown in Figure 1).

To address these challenges, we propose to apply a graph neural network to generate multimodal features for each aphasia type, enabling the acquisition of rich semantics across modalities (Banarescu et al., 2013). Due to the heterogeneity among multimodalities in clinical datasets (Pei et al., 2023), a unique graph structure can help distinguish diverse patterns (Zhang et al., 2022) by learning the correlation between speech and the corresponding gestures of PWA with different aphasia.

Specifically, we construct a heterogeneous network that represents the relationships between speech (particularly including disfluency-related keywords and acoustic information) and gesture modalities based on their co-occurrence by using data from AphasiaBank (Forbes et al., 2012; MacWhinney et al., 2011), a shared database for aphasia research. Then, Speech-Gesture Graph Encoder (§4.2) extracts three node embeddings for disfluency-related keywords, audio, and gesture tokens by aggregating information from different sources. Before fusing the modalities, the Gesture-aware Word Embedding Layer (§4.3) generates textual representations sensitive to gesture informa-

tion by adjusting the weights of pre-trained word embeddings with the refined representations of disfluency tokens. Consequently, a multimodal Fusion Encoder (§4.4) is applied to incorporate aphasia-type-specific multimodal representations to predict the final aphasia type (§4.5).

The extensive experiments show that our model performs better than the prior methods in detecting aphasia types. We find that applying the GNN can effectively generate multimodal features by capturing relations between speech and gesture information, enhancing performance. Our analysis reveals that gesture features play more critical roles in predicting aphasia types than acoustic features, implying that gesture expression is a unique attribute of PWA with different types. We exemplify that the qualitative analysis based on the proposed model can help clinicians understand aphasia patients more comprehensively, helping to provide timely interventions. To the best of our knowledge, this is the first attempt that uses gesture and speech information for automatic aphasia types detection.

## 2 Related Work

**Aphasia analysis and detection.** To identify the pathological symptoms shown in a narrative speech of PWA, researchers have focused on linguistic features (e.g., word frequency, Part-of-Speech (Le et al., 2018), word embeddings (Qin et al., 2019a)), and acoustic features (e.g., filler words, pauses, the number of phones per word (Le and Provost, 2016; Qin et al., 2019b)). With the advances in automated speech recognition (ASR) that can make the transcription of aphasic speech into text (Radford et al., 2022; Baevski et al., 2020), there have been end-to-end approaches that do not require explicit feature extraction in assessing patients with aphasia (Chatzoudis et al., 2022; Torre et al., 2021). While these works reveal valuable insight into detecting aphasia, little attention has been paid to identifying the types of aphasia, which can be crucial for proper treatment procedures. Considering the importance of understanding gesture patterns for identifying the types of aphasia (Preisig et al., 2018), we propose a multimodal aphasia type prediction model using both speech and gesture information.

**Multimodal learning for detecting language impairment.** Multimodal language analysis helps to understand human communication by integrating information from multiple modalities for tasks such as sentiment analysis (Zadeh et al., 2017) and

emotion recognition (Yoon et al., 2022). However, previous studies simply concatenated features to identify language impairment in speech data (Rohanian et al., 2021; Balagopalan et al., 2020), which lacks comprehension of the complex connections between modalities (Cui et al., 2021; Syed et al., 2020). To capture interconnections between modalities, recent studies used Transformer-based multimodal models (Lin et al., 2022; Rahman et al., 2020a) that can extract contextual information across modalities, utilizing factorized co-attention (Cheng et al., 2021), self-attention (Hazari et al., 2020), or cross-modal attention (Tsai et al., 2019). While the prior work tended to capture a single link between modalities, e.g., linking the ‘happy’ (linguistic modality) to a smiling face (visual modality) (Yang et al., 2021; Tsai et al., 2019), little attention has been paid to learning multiple links across the modalities, which can be crucial in aphasia type detection. As shown in Figure 1, speech and gesture modalities may have multiple links across the different aphasia types. Hence, to distinguish aphasia types, we propose to apply a graph neural network to generate multimodal features for each aphasia by learning the correlation between speech and gesture patterns of PWA.

### 3 Aphasia Dataset

**Data Collection** We sourced our dataset from the AphasiaBank (MacWhinney et al., 2011; Forbes et al., 2012), a shared database used by clinicians for aphasia research; the corpus information is summarized in Table 6 in Appendix. The dataset provides video recordings of the language evaluation test process between a pathologist and a subject, which also includes human-annotated transcriptions and subjects’ demographic information. Among the evaluation tests, we chose the Cinderella Story Recall task (Bird and Franklin, 1996), where pictures from the Cinderella storybook are shown to participants, who are then asked to recall and retell the story spontaneously. The test has been proven as a helpful tool that can offer valuable insights into a subject’s speech and language skills (Illes, 1989).

Each data is categorized into one of four types: *Control*, *Fluent*, *Non-Comprehension*, *Non-Fluent*, based on the ability to auditory comprehension and fluency skills, as shown in Table 1. Due to the limited amount of data available for training, specific types of aphasia, such as Global aphasia and Transcortical mixed aphasia, are excluded during

Table 1: Summary of data statistics of the aligned modalities with 50 tokens for each user. (✓: impaired, ✗: not impaired).

Labels	Impaired		Aphasia Types	Data Statistics		
	Flu.	Com.		Subj.	Samp.	Dur. (s)
Ctrl	✗	✗	Control	194	1,815	17.14
Flu	✗	✗	Anomic	143	927	31.80
			Conduction	62	424	26.27
Non Com.	✗	✓	Sensory Wernicke	1	3	15.83
			Motor Broca	26	188	24.68
Non Flu.	✓	✗	Motor Broca	8	23	43.01
			Broca	73	271	34.75
Total				507	3,651	23.78

data preprocessing.

**Data Preprocessing** We utilize Whisper (Radford et al., 2022), a popular ASR model, to generate automated transcriptions. Unlike previous ASR systems focusing on transcribing clean speech (Torre et al., 2021), Whisper can capture filler words (e.g., um, uh) and unintelligible disfluency words (e.g., [\*]) at the token level. As depicted in Table 8 in Appendix, the Word Error Rate (WER) results show that the average WER for all participants is comparable to the previous research (Weiner et al., 2017). Furthermore, our research reveals that the text preprocessing results in a decrease in WER due to the frequent presence of fillers and disfluencies in the text of PWA, except for those with non-fluent aphasia types (e.g., *Non-Fluent*).

We then align the text tokens with corresponding gesture and audio tokens using the provided timestamps (Louradour, 2023). We extract the first frame (1 FPS) as a representative image for the gesture tokens. To augment the dataset, we chunk the aligned modalities with 50 tokens for each user except any segment less than 3 seconds long, as shown in Figure 1. Note that we exclude the segments of the interviewer in the video recordings since their subjective reactions can potentially affect the patient’s performance (Parveen and Santhanam, 2021; Qin et al., 2018b).

Finally, the dataset consists of 507 subjects and their 3,651 aligned modalities, with an average duration of 23.78 seconds, as shown in Table 1.

### 4 Aphasia Type Detection

Figure 2 illustrates the overall architecture of the proposed model for detecting aphasia types. The model comprises four main components: Speech-Gesture Graph Encoder (§4.2), Gesture-aware Word Embedding Layer (§4.3), Multimodal Fusion Encoder (§4.4), and Aphasia Type Prediction Decoder (§4.5).

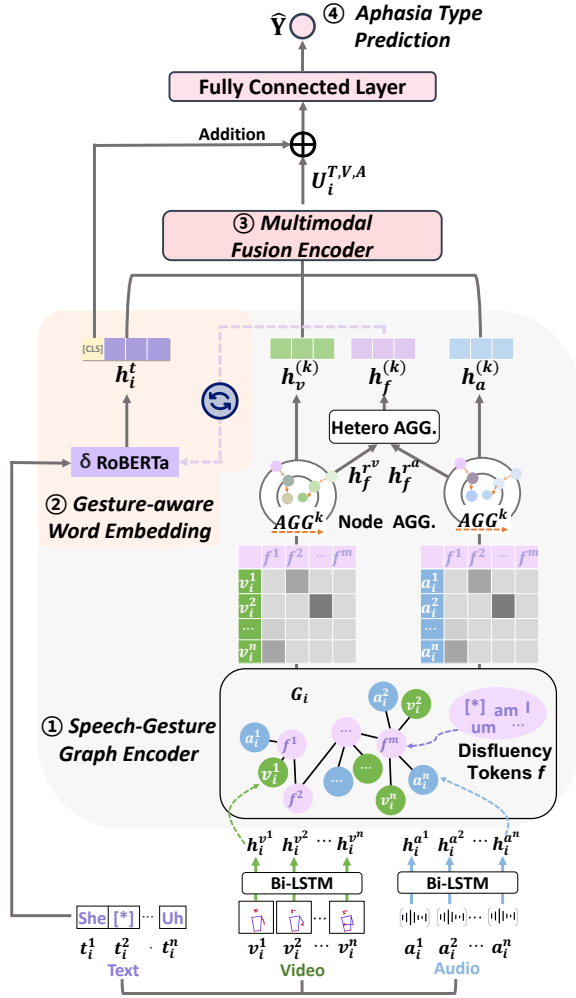


Figure 2: The overall architecture of the proposed model: ① Speech-Gesture Graph Encoder (§4.2), ② Gesture-aware Word Embedding Layer (§4.3), ③ Multimodal Fusion Encoder (§4.4), and ④ Aphasia Type Prediction Decoder (§4.5).

#### 4.1 Problem Statement

Suppose we have a set of aphasia dataset  $C = \{c_i\}_{i=1}^{|C|}$ ,  $c_i$  is structured on an  $n$  length of sequences, including text tokens ( $t_i^n$ ), gesture tokens ( $v_i^n$ ), and audio tokens ( $a_i^n$ ) as described in Figure 1, which can be represented as  $c_i = (t_i^n, v_i^n, a_i^n)$ . Then, the proposed model is defined as a multi-class classification problem that classifies an aphasia data  $c_i$  into an Aphasia type  $y_i \in \{\text{Control}, \text{Fluent}, \text{Non-Comprehension}, \text{Non-Fluent}\}$ .

#### 4.2 Speech-Gesture Graph Encoder

We propose a Speech-Gesture Graph Encoder that can generate multimodal features specific to each aphasia type by learning the correlation between speech and gesture patterns in identifying the aphasia types.

#### 4.2.1 Heterogeneous Graph Construction

In a preliminary analysis, we observed statistical differences between words, especially disfluency-related keywords, and aligned gesture features across different aphasia types (see Table 11 in Appendix). Based on the findings, we construct a set of heterogeneous graphs  $\mathbb{G} = \{G_1, G_2, \dots, G_i\}$  for  $c_i$  that represents the relationships between disfluency-related keywords and multimodalities (i.e., gesture, audio) based on their co-occurrence. Note that we use the same disfluency tokens for each graph in  $\mathbb{G}$  to capture the differences between users with different aphasia types. Disfluency keywords are extracted based on their frequency in ASR transcriptions, as shown in Table 9 in Appendix. Unlike previous approaches (Day et al., 2021), we do not remove ‘stop words’ because most disfluency-related words are associated with such ‘stop words,’ which are typically filtered out in text classification tasks. Formally, each graph is defined with the set of disfluency nodes  $V_f$ , which are connected to aligned gesture  $V_v$  and audio  $V_a$  nodes in aligned multimodal data  $c_i$  as follows.

$$G_i = (V_f, V_v, V_a, E_{fv}, E_{fa}) \quad (1)$$

**Textual Representation.** In order to extract the representation of disfluency node in  $V_f$ , we use the pre-trained RoBERTa (Liu et al., 2019) that is a pre-training language model shows a robust performance across various NLP tasks. After tokenizing the set of words  $\{f_i^m\}_{i=1}^{|m|}$  into  $e_i^f$ , we encode them as follows.

$$h^f = \text{RoBERTa}(e^f) \in \mathbb{R}^{m \times d_t} \quad (2)$$

where  $d_t$  is the dimension of the textual feature. If any disfluency keywords are not included in the vocabulary of the pre-trained tokenizer, we add new tokens to represent these keywords.

**Visual Representation.** To utilize the gesture information for gesture nodes  $V_v$ , we extract the pose landmarks using MediaPipe<sup>2</sup> (Lugaresi et al., 2019) API that generates body pose landmarks, providing image-based 3-dimensional coordinates. Since our video data captures participants seated, we exclude the lower body keypoints and leverage the 23 upper body keypoints. Visual feature  $e_i^v$  is fed into a bidirectional LSTM to derive context representation, reflecting the dynamic nature of an individual’s gestures. Finally, the hidden state vectors are concatenated as follows.

<sup>2</sup><https://developers.google.com/mediapipe>

$$h_i^v = [\overrightarrow{LSTM}(e_i^v, h_{i-1}^v), \overleftarrow{LSTM}(e_i^v, h_{i+1}^v)] \quad (3)$$

**Acoustic Representation.** For audio feature extraction, we use OpenSmile (Eyben et al., 2010), an open-source audio processing toolkit, with extended Geneva Minimalistic Acoustic Parameter Set (eGeMAPS) (Eyben et al., 2015). We extract 25 low-level acoustic descriptors (LLDs) in each second, including loudness, MFCCs (Mel-frequency cepstral coefficients), and other relevant features. We then average the values of all 25 features to obtain audio features  $e_i^a$ . After that, the audio hidden state vectors are extracted, adopting the same approach for extracting visual features as follows.

$$h_i^a = [\overrightarrow{LSTM}(e_i^a, h_{i-1}^a), \overleftarrow{LSTM}(e_i^a, h_{i+1}^a)] \quad (4)$$

#### 4.2.2 Cross-relation Aggregation

To update the features of the target node  $V$ , we adopt GraphSAGE (Hamilton et al., 2017), a widely used GNN model that supports batch training without requiring updates across the entire graph. This recursive approach involves updating the embeddings of each node by aggregating information from its immediate neighbors using an aggregation function at each search depth ( $k$ ). Specifically, the representation  $h_V^k$  of node  $V$  is updated by combining  $h_V^{k-1}$  with information obtained from  $h_{\mathcal{N}(V)}^k$ , which represents the neighboring nodes of  $V$  at step  $k$ . The initial output is  $h_V^0 = h_V$ , and the series of updating processes are defined as follows.

$$h_{\mathcal{N}(V)}^{(k)} = \text{NodeAGG}^k \left( \{h_u^{k-1}, \forall u \in \mathcal{N}(V)\} \right) \quad (5)$$

$$h_V^{(k)} = \sigma \left( W^k \cdot (h_V^{k-1} \oplus h_{\mathcal{N}(V)}^k) \right) \quad (6)$$

If the target node  $V$  has multiple relations from different types of source nodes  $\{r_j\}_{j=1}^{|\mathcal{N}(v)|} \in \mathcal{N}(v)$ ,  $V$  has heterogeneous representations as follows.

$$h_V^{(k)} = [h_V^{r_1}, h_V^{r_2}, \dots, h_V^{r_j}] \quad (7)$$

where  $j$  is the number of source node types among the neighbors of target node  $V$ . Since latent information from distinct source node embeddings can affect the target node representation differently, we aim to aggregate the fine-grained interplay between them without losing valuable knowledge by maintaining independent distributions. Finally, we derive a feature of node  $V$  at step  $k$  as follows.

$$\hat{h}_V^{(k)} = \text{HeteroAGG}^K \left( h_V^{(k)} \right) \quad (8)$$

In this way, three aggregated representations for disfluency, gesture, and audio tokens, respectively, are obtained as follows.

$$H_i = \{\hat{h}_f^{(k)}, \hat{h}_a^{(k)}, \hat{h}_v^{(k)}\} \quad (9)$$

#### 4.3 Gesture-aware Word Embedding Layer

To obtain textual features  $h_i^t$  sensitive to gesture information, we update the pre-trained RoBERTa word embedding weights (Liu et al., 2019) with updated disfluency representations  $\hat{h}_f^{(k)}$  as follows.

$$\hat{h}_f^{(k)} = \delta \text{RoBERTa}(e^f) \in \mathbb{R}^{m \times d_t} \quad (10)$$

$$h_i^t = \delta \text{RoBERTa}(e_i^t) \in \mathbb{R}^{n \times d_t} \quad (11)$$

Subsequently, the final multimodal representation for  $c_i$  is derived as follows.

$$\hat{H}_i = \{h_i^t, \hat{h}_a^{(k)}, \hat{h}_v^{(k)}\} \quad (12)$$

#### 4.4 Multimodal Fusion Encoder

To fuse multimodal representations, we utilize a Multimodal Transformer (Tsai et al., 2019) that effectively integrates multimodal features by capturing contextual information. We employ two cross-attention layers and a self-attention mechanism for generating each modality feature as shown Figure 7 in Appendix. For example, when the model generates a textual feature, each layer (i.e., (V→T), (A→T)) uses the visual and acoustic representations as the key/value pairs, respectively, and textual representation as the query vector. After concatenating two features from each layer, a self-attention Transformer fuses them to generate cross-modal representation  $U^T$ . Next, the model concatenates three cross-modal features (i.e.,  $U^T, U^V, U^A$ ) to derive the final multimodal representation  $U^{TVA}$  as follows (See Tsai et al. (2019) for more details).

$$U_i^{TVA} = U_i^T \oplus U_i^V \oplus U_i^A \quad (13)$$

Finally, we add the pooled embeddings of [CLS] token in  $h_i^t$  and the  $U^{TVA}$  as follows.

$$\hat{U}_i = U_i^{TVA} + h_i^{t, \text{CLS}} \quad (14)$$

#### 4.5 Aphasia Type Prediction

To predict the types of aphasia for  $c_i$ , the final prediction vector is generated as follows.

$$\hat{y} = \mathcal{F}(\text{ReLU}(\mathcal{F}(\hat{U}_i))) \quad (15)$$

where  $\mathcal{F}$  is a fully-connected layer and  $\text{ReLU}$  is an activation function. Finally, the cross-entropy

loss is calculated using the probability distribution  $y$  and classification score  $\hat{y}$  obtained as follows.

$$\mathcal{L} = -\frac{1}{b} \sum_{i=1}^b y_i \log \hat{y}_i \quad (16)$$

where  $b$  is the batch size.

## 5 Experiments

### 5.1 Experimental Settings

Table 10 in Appendix shows that we split the dataset into the train and test sets with an 8:2 ratio. In all our experiments, we ensure that users in the test set are entirely disjoint and do not overlap with those in the training set. For reproducibility, detailed experimental settings are summarized in Appendix B.1.

### 5.2 Baselines

To conduct extensive performance comparisons, we consider two categories of baseline methods: (i) aphasia & dementia detection models and (ii) multimodal fusion baselines. A detailed explanation of the baselines is summarized in Appendix B.2.

**Aphasia & Dementia Detection Baselines.** Since predicting aphasia types has yet to be explored, we compare the approaches from the related tasks that only detect the presence or absence of aphasia. Additionally, we compare the popular models for dementia detection: (i) Logistic Regression (LR) (Cui et al., 2021; Syed et al., 2020), (ii) Support Vector Machines (SVM) (Qin et al., 2018b; Rohanian et al., 2021), (iii) Random Forest (RF) (Cui et al., 2021; Balagopalan et al., 2020), (iv) Decision Tree (DT) (Qin et al., 2018b; Balagopalan and Novikova, 2021), and (v) AdaBoost (Cui et al., 2021).

**Multimodal Fusion Baselines.** We compare the proposed model with the following four existing multimodal fusion methods: (i) MulT (Tsai et al., 2019), (ii) MISA (Hazarika et al., 2020), (iii) MAG (Rahman et al., 2020b), and (iv) SP-Transformer (Cheng et al., 2021).

## 6 Results

### 6.1 Model Performance

Table 2 shows the weighted average F1-score of the baselines and the proposed model across the aphasia types. The proposed model outperforms all the baselines (F1 84.2%) regardless of the aphasia types. Specifically, deep learning-based multimodal fusion models perform better than models that simply concatenate multimodal features in

Table 2: Comparison of performance between the proposed model and baseline models, with results averaged over a Group Stratified 5-fold cross-validation. Results marked with an asterisk (\*) indicate statistical significance compared to MAG ( $p < 0.05$ ) according to the Wilcoxon’s signed rank test.

Model		Label (F1-score)				
		Total	Ctrl	Flu	Non Com.	Non Flu.
Aphasia& Dementia Detection	SVM	0.338	0.670	0.000	0.000	0.000
	RF	0.742	0.871	0.719	0.000	0.400
	DT	0.688	0.824	0.652	0.090	0.283
	LR	0.655	0.773	0.696	0.000	0.000
	AdaBoost	0.719	0.882	0.662	0.000	0.303
Fusion	MISA	0.761	0.899	0.741	0.000	0.349
	MulT	0.761	0.885	0.750	0.000	0.410
	MAG	0.725	0.838	0.698	0.000	0.514
	SP-Trans.	0.756	0.893	0.742	0.000	0.324
Ours	30 Tok.	0.732	0.906	0.676	<b>0.303</b>	0.446
	<b>50 Tok.</b>	<b>0.842*</b>	<b>0.949*</b>	<b>0.840*</b>	0.125	<b>0.530</b>

Table 3: Ablation study to examine the effectiveness of §4.2 Speech-Gesture Graph Encoder and §4.4 Multimodal Fusion Encoder.

Component		Prec	Rec	F1
Node agg.	LSTM	0.777	0.790	0.780
	Mean	0.722	0.743	0.722
	Pool	0.781	0.807	0.787
	<b>BiLSTM</b>	<b>0.837</b>	<b>0.852</b>	<b>0.842</b>
Hetero agg.	Mean	0.785	0.763	0.771
	Sum	0.759	0.774	0.761
	Max	0.794	0.803	0.783
	<b>Min</b>	<b>0.837</b>	<b>0.852</b>	<b>0.842</b>
Fusion	Concat	0.746	0.609	0.568
	Multiply	0.776	0.808	0.784
	Add	0.789	0.793	0.751
	SP-Trans.	0.757	0.781	0.758
	<b>MulT</b>	<b>0.837</b>	<b>0.852</b>	<b>0.842</b>

predicting aphasia types. We observe that the proposed model can relatively accurately predict minorities such as *Non – Comprehension* (N=191) than other baselines. We also investigate how the number of tokens  $n$  decided in creating an aligned multimodal dataset (Figure 1) affects the model performance. As demonstrated in Table 2, we find that the F1-score is higher for the model using 50 tokens than 30 tokens, which indicates the importance of comprehending longer sequences for accurate prediction of aphasia types. While the utilization of 30 tokens improves the performance of *Non – Comprehension*, we attribute this improvement to the larger size of the dataset based on 30 tokens, as indicated in Table 7 in the Appendix.

### 6.2 Ablation Study

We perform an ablation study to examine the effectiveness of each component of the proposed model. **Analysis on Model Components.** As described

in Table 3, the model performance significantly improves when we use the BiLSTM node aggregator (Tang et al., 2020). Given that our dataset is structured on a sequence level, RNN-based models exhibit higher performance with their capacity to capture long-term dependencies. Also, the Min heterogeneous aggregate function (Wang et al., 2019) can effectively learn relationships between sources from multiple modalities. We also compare the multimodal fusion models, including Transformer-based multimodal fusion models (Tsai et al., 2019; Cheng et al., 2021) as a Multimodal Fusion Encoder. As shown in Table 3, MulT (Tsai et al., 2019) model performs better at 84.2% of F1-score, suggesting its capability to generate a more informative multimodal representation.

**Analysis on Different Modalities.** To analyze the significance of each modality in detecting aphasia types, we perform an analysis of unimodal models trained with each modality. For unimodal aphasia type detection, we solely utilized the unimodal Transformer encoder. As shown in Table 4, the model trained with text features performs better (F1 70.0%). This indicates that linguistic features are more informative for identifying language impairment disorders (Cui et al., 2021; Chen et al., 2021). Additionally, visual features outperform acoustic features (F1 62.9%), suggesting that PWA exhibit distinct characteristics in their gesture expression. When constructing a graph  $G$ , employing only the edge  $E_{fv}$  between disfluency and gesture tokens results in higher performance (F1 77.3%) compared to using the edge  $E_{fa}$  between disfluency and audio tokens (F1 74.7%), as described in Table 4. However, considering all three modalities together shows the best performance, which reveals that learning linguistic features along with visual and acoustic characteristics and their relations is more effective than relying solely on one modality.

**Analysis on Speech-Gesture Graph Encoder.** We next explore the effectiveness of the proposed Speech-Gesture Graph Encoder to understand how the multimodal features specific to each aphasia type are helpful in performance. We first find that using multimodal features from the graph encoder helps to improve prediction performance (F1 79.2%) compared to without graph encoder (F1 76.5%), as described in Table 4. We attribute this to the strength of the graph neural network model, which can learn better representations from cross-modal relations. Also, the performance notably

Table 4: Comparison of the impact of §4.2 Speech-Gesture Graph Encoder and §4.3 Gesture-aware Word Embedding Layer on each modality.

Component			Metrics		
Graph Encoder	Update Embed.	Modality	Prec	Rec	F1
✗	✗	Text	0.692	0.727	0.700
✗	✗	Acoustic	0.455	0.566	0.501
✗	✗	Visual	0.591	0.689	0.629
✗	✗	T+V+A	0.749	0.786	0.765
✓	✗	T+V+A	0.774	0.814	0.792
✓	✓	T+V	0.767	0.781	0.773
✓	✓	T+A	0.771	0.740	0.747
✓	✓	T+V+A	<b>0.837</b>	<b>0.852</b>	<b>0.842</b>

improves when using refined word embeddings (F1 84.2%) compared to just pre-trained word embeddings (F1 79.2%). This implies that gesture-sensitive text features can help the multimodal fusion encoder to assign different weights to each modality considering the meaning of words.

We further conduct experiments to determine the optimal number  $m$  of disfluency token nodes  $V_f$  in the graph  $G$ , ranging from 50 to 300. Figure 3 illustrates the weighted average F1/Precision/Recall scores for identifying aphasia types across the different  $m$  disfluency keywords. The performance improves as more keywords are included, but no further enhancement is observed beyond 150 keywords. However, our analysis demonstrates that using 100 keywords produces better results compared to using 300 keywords. We believe that extracting important disfluency keywords will result in improved outcomes. In our future work, we plan to collaborate with clinical experts, including speech-language pathologists and neurologists, to acquire valuable clinical insights and guidance.

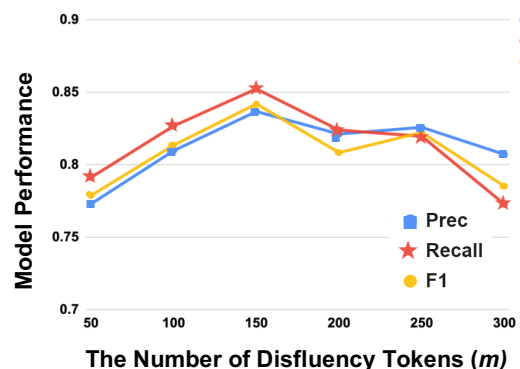


Figure 3: Performance of the model by the number of disfluency tokens ( $m$ ).

**Analysis on Different Gender.** Earlier clinical research indicates that different gender is associated with aphasia severity, including communica-

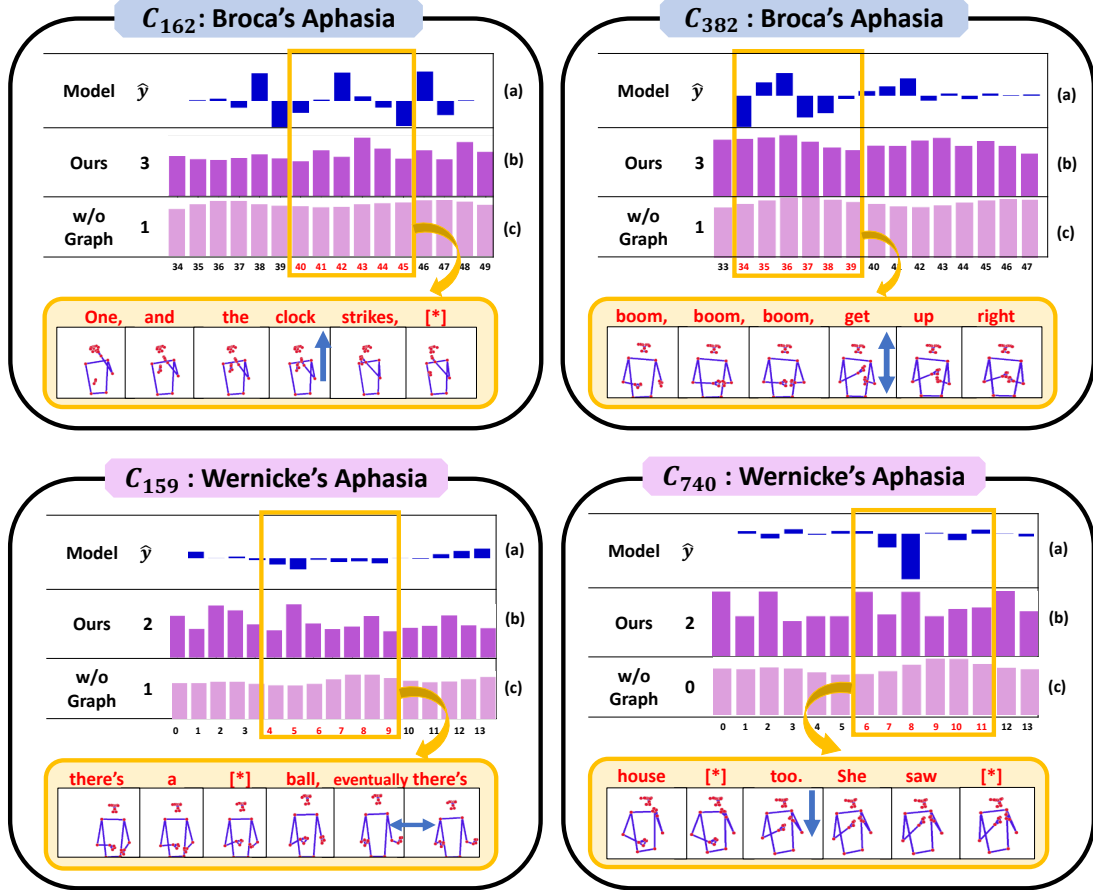


Figure 4: Visualization of the crossmodal attention matrix from the  $V \rightarrow L$  network of the Multimodal Fusion Encoder for the proposed model with (b) or without (c) the speech-gesture graph encoder. (a) presents the differences in the spatial position of the right wrist’s landmark compared to the previous frame, where positive and negative values indicate upward/rightward and downward/leftward movements.

Table 5: Gender differences in the model performance.

Train	Test	Prec	Rec	F1
Both	Both	<b>0.837</b>	<b>0.852</b>	<b>0.842</b>
	Female	0.889	0.890	0.885
	Male	0.795	0.820	0.805
Female	Both	0.718	0.761	0.724
	Female	0.757	0.801	0.772
	Male	0.668	0.727	0.683
Male	Both	0.795	0.771	0.777
	Female	0.805	0.758	0.773
	Male	0.794	0.782	0.785

tion impairment and lower scores on specific subtests (Sharma et al., 2019). To validate this observation, we train and validate our model using separate datasets of either male or female participants (Table 5). The model performs better when trained on the male dataset (F1 77.7%) than the female dataset (F1 72.4%), despite a larger training size from females (Table 10). These findings suggest that the linguistic impairment caused by aphasia is more pronounced in male patients, as reported in previous studies (Yao et al., 2015). Thus, we believe the model can learn linguistic impairment markers better when trained with the male dataset.

### 6.3 Qualitative Analysis

In this section, we perform a qualitative analysis on four representative cases involving different types of aphasia, especially Broca’s (i.e.,  $c_{162}$ ,  $c_{382}$ ) and Wernicke’s aphasia (i.e.,  $c_{159}$ ,  $c_{740}$ ). As shown in Figure 4, we compare the cross-modal attention matrix from the  $V \rightarrow L$  network of the Multimodal Fusion Encoder in the proposed model with or without the speech-gesture graph encoder. Each attention weight can be interpreted as the relevance of the visual and the textual features. Note that Figure 6 in Appendix visualizes the standard deviation of pose landmarks of individuals, which reveals that the Non-Fluent type (e.g., Broca’s aphasia) exhibits a broader range of activity compared to the Non-Comprehension type (e.g., Wernicke’s aphasia) (Lanyon and Rose, 2009).

We find that the model without a graph encoder assigns the same attention regardless of the aphasia types when significant physical actions are displayed. However, our proposed model can predict Broca’s aphasia (i.e.,  $c_{162}$ ,  $c_{382}$ ) by assigning higher attention weights if meaningful motions are cap-

tured. For example,  $c_{162}$  points the index finger to express the ‘clock’ and  $c_{382}$  indicates upward movements during phrases like ‘get up’. This implies that PWA with Broca’s aphasia leverage gestures as an additional means of communication (Preisig et al., 2018; de Kleine et al., 2023), and the proposed model can accurately recognize the meaning of gestures associated with the text. By contrast, in the cases of Wernicke’s aphasia ( $c_{159}, c_{740}$ ), where motions are commonly small, the model assigns higher attention scores to any noticeable motion change, despite the meaning of the movement.

We believe the proposed model with a speech-gesture graph encoder can effectively generate aphasia type-specific multimodal features for predicting aphasia types, as demonstrated in our case study. Thus, the proposed model can be used for screening and identifying individuals with aphasia to prioritize early intervention for clinical support.

## 7 Conclusion

In this paper, our approach utilizing GNNs proves effective in generating multimodal features specific to each aphasia type for predicting aphasia types. The extensive experiments demonstrated state-of-the-art results, with visual features outperforming acoustic features in predicting aphasia types. We plan to provide the codes for reproducibility, facilitating further research in this area. The qualitative analysis offered valuable insights that can enhance clinicians’ understanding of aphasia patients, leading to more comprehensive assessments and timely interventions. Overall, our research contributes to the field of aphasia diagnosis, highlighting the importance of using multimodal information and graph neural networks. We believe our findings will drive advancements in speech and language therapy practices for individuals with aphasia.

## Ethics Statement

We sourced the dataset from AphasiaBank with Institutional Review Board (IRB) approval<sup>3</sup> and strictly follow the data sharing guidelines provided by TalkBank<sup>4</sup>, including the Ground Rules for all TalkBank databases based on American Psychological Association Code of Ethics (Association et al., 2002). Additionally, our research adheres to the five core issues outlined by TalkBank in accordance with the General Data Protection Regulation

(GDPR) (Regulation, 2018). These issues include addressing commercial purposes, handling scientific data, obtaining informed consent, ensuring deidentification, and maintaining a code of conduct. Considering ethical concerns, we did not use any photographs and personal information of the participants from the AphasiaBank.

## Limitations

First, traditional aphasia classification schemes, such as the WAB (Western Aphasia Battery) (Kertesz, 2007), have faced criticism because patients’ symptoms often do not fit into a single type, and there is overlap between the different classes (Caramazza, 1984; Swindell et al., 1984). However, the WAB still offers a means to categorize patients based on their most prominent symptoms. Furthermore, datasets labeled using the WAB scheme are essential for studies that rely on methods requiring a substantial amount of training data.

Second, the previous study highlighted the potential of identifying repetitive mouth patterns to detect speech impairments (Einfalt et al., 2019). However, capturing mouth landmarks on the subjects was challenging due to the considerable distance at which the videos were recorded in the AphasiaBank dataset. Considering the significant role of mouth information in human communication (Busso et al., 2004), we anticipate that incorporating mouth information in conjunction with gesture information will improve performance.

Additionally, we utilized computational methods to extract disfluency-related keywords from frequent occurrences, which were then used for constructing the graph. However, our analysis in Figure 3 demonstrated that using 100 tokens produced better results compared to using 300 tokens. Consequently, we believe that extracting significant disfluency tokens guided by expert advice will result in improved outcomes. In our future work, we intend to collaborate with clinical experts, including speech-language pathologists and neurologists, to acquire valuable clinical insights and guidance.

## Acknowledgments

This research was supported by the Ministry of Education of the Republic of Korea and the National Research Foundation (NRF) of Korea (NRF-2022S1A5A8054322) and the National Research Foundation of Korea grant funded by the Korea government (MSIT) (No. 2023R1A2C2007625).

<sup>3</sup>SKKU2022-11-039

<sup>4</sup><https://talkbank.org/share/ethics.html>

## References

- Martin L Albert, Robert W Sparks, and Nancy A Helm. 1973. Melodic intonation therapy for aphasia. *Archives of neurology*, 29(2):130–131.
- American Psychological Association et al. 2002. Ethical principles of psychologists and code of conduct. *American psychologist*, 57(12):1060–1073.
- Alexei Baevski, Yuhao Zhou, Abdelrahman Mohamed, and Michael Auli. 2020. wav2vec 2.0: A framework for self-supervised learning of speech representations. *Advances in neural information processing systems*, 33:12449–12460.
- Aparna Balagopalan, Benjamin Eyre, Frank Rudzicz, and Jekaterina Novikova. 2020. To bert or not to bert: Comparing speech and language-based approaches for alzheimer’s disease detection. *Proc. Interspeech 2020*, pages 2167–2171.
- Aparna Balagopalan and Jekaterina Novikova. 2021. [Comparing Acoustic-Based Approaches for Alzheimer’s Disease Detection](#). In *Proc. Interspeech 2021*, pages 3800–3804.
- Laura Banarescu, Claire Bonial, Shu Cai, Madalina Georgescu, Kira Griffitt, Ulf Hermjakob, Kevin Knight, Philipp Koehn, Martha Palmer, and Nathan Schneider. 2013. Abstract meaning representation for sembanking. In *Proceedings of the 7th linguistic annotation workshop and interoperability with discourse*, pages 178–186.
- Helen Bird and Sue Franklin. 1996. Cinderella revisited: A comparison of fluent and non-fluent aphasic speech. *Journal of neurolinguistics*, 9(3):187–206.
- Mary Boyle. 2013. [Aphasiabank english protocol pwa msu corpus](#).
- Paul Broca et al. 1861. Remarks on the seat of the faculty of articulated language, following an observation of aphemia (loss of speech). *Bulletin de la Société Anatomique*, 6:330–57.
- Carlos Busso, Murtaza Bulut, Chi-Chun Lee, Abe Kazemzadeh, Emily Mower, Samuel Kim, Jeanette N Chang, Sungbok Lee, and Shrikanth S Narayanan. 2008. Iemocap: Interactive emotional dyadic motion capture database. *Language resources and evaluation*, 42:335–359.
- Carlos Busso, Zhigang Deng, Serdar Yildirim, Murtaza Bulut, Chul Min Lee, Abe Kazemzadeh, Sungbok Lee, Ulrich Neumann, and Shrikanth Narayanan. 2004. Analysis of emotion recognition using facial expressions, speech and multimodal information. In *Proceedings of the 6th international conference on Multimodal interfaces*, pages 205–211.
- Katy Bynek. 2013. [Aphasiabank english protocol pwa acwt corpus](#).
- Gilson Capilouto. 2008. [Aphasiabank english controls capilouto corpus](#).
- Alfonso Caramazza. 1984. The logic of neuropsychological research and the problem of patient classification in aphasia. *Brain and language*, 21(1):9–20.
- Gerasimos Chatzoudis, Manos Plitsis, Spyridoula Stamouli, Athanasia-Lida Dimou, Athanasios Katsamanis, and Vassilis Katsouros. 2022. Zero-shot cross-lingual aphasia detection using automatic speech recognition. *arXiv preprint arXiv:2204.00448*.
- Jun Chen, Jieping Ye, Fengyi Tang, and Jiayu Zhou. 2021. Automatic detection of alzheimer’s disease using spontaneous speech only. In *Proceedings of Conference of the International Speech Communication Association (Interspeech 2021)*.
- Junyan Cheng, Iordanis Fostropoulos, Barry Boehm, and Mohammad Soleymani. 2021. Multimodal phased transformer for sentiment analysis. In *Proceedings of the 2021 Conference on Empirical Methods in Natural Language Processing*, pages 2447–2458.
- Melinda Corwin. 2013. [Aphasiabank english protocol pwa star corpus](#).
- Xia Cui, Amila Gamage, Terry Hanley, and Tingting Mu. 2021. Identifying indicators of vulnerability from short speech segments using acoustic and textual features. In *Interspeech*, pages 1569–1573.
- Marjory Day, Rupam Kumar Dey, Matthew Baucum, Eun Jin Paek, Hyejin Park, and Anahita Khojandi. 2021. Predicting severity in people with aphasia: A natural language processing and machine learning approach. In *2021 43rd Annual International Conference of the IEEE Engineering in Medicine & Biology Society (EMBC)*, pages 2299–2302. IEEE.
- Naomi de Kleine, Miranda L Rose, Michael Weinborn, Robert Knox, and Nicolas Fay. 2023. Does gesture improve the communication success of people with aphasia?: A systematic review. *Aphasiology*, pages 1–25.
- Michael Dean. 2021. [Aphasiabank english protocol pwa ucl corpus](#).
- Moritz Einfalt, Rainer Lienhart, Matthew Lee, and Lyndon Kennedy. 2019. Detecting speech impairments from temporal visual facial features of aphasia patients. In *2019 IEEE Conference on Multimedia Information Processing and Retrieval (MIPR)*, pages 103–108. IEEE.
- Hanane El Hachoui, Evy G Visch-Brink, Lonke ML de Lau, Mieke WME van de Sandt-Koenderman, Femke Nouwens, Peter J Koudstaal, and Diederik WJ Dippel. 2017. Screening tests for aphasia in patients with stroke: a systematic review. *Journal of neurology*, 264:211–220.
- Roberta J Elman. 2011. Starting an aphasia center? In *Seminars in speech and language*, volume 32, pages 268–272. © Thieme Medical Publishers.

- Roberta J Elman. 2016. Aphasia centers and the life participation approach to aphasia. *Topics in Language Disorders*, 36(2):154–167.
- Florian Eyben, Klaus R Scherer, Björn W Schuller, Johan Sundberg, Elisabeth André, Carlos Busso, Laurence Y Devillers, Julien Epps, Petri Laukka, Shrikanth S Narayanan, et al. 2015. The geneva minimalistic acoustic parameter set (gemaps) for voice research and affective computing. *IEEE transactions on affective computing*, 7(2):190–202.
- Florian Eyben, Martin Wöllmer, and Björn Schuller. 2010. Opensmile: the munich versatile and fast open-source audio feature extractor. In *Proceedings of the 18th ACM international conference on Multimedia*, pages 1459–1462.
- Yasmeen Farooqi-Shah and Lisa Milman. 2018. Comparison of animal, action and phonemic fluency in aphasia. *International journal of language & communication disorders*, 53(2):370–384.
- Margaret M Forbes, Davida Fromm, and Brian MacWhinney. 2012. Aphasiabank: A resource for clinicians. In *Seminars in speech and language*, volume 33, pages 217–222. Thieme Medical Publishers.
- Kathleen C Fraser, Jed A Meltzer, Naida L Graham, Carol Leonard, Graeme Hirst, Sandra E Black, and Elizabeth Rochon. 2014. Automated classification of primary progressive aphasia subtypes from narrative speech transcripts. *cortex*, 55:43–60.
- Julius Fridriksson. 2013. [Aphasiabank english protocol pwa fridriksson corpus](#).
- Kathryn Garrett. 2013. [Aphasiabank english protocol pwa garrett corpus](#).
- William L Hamilton, Rex Ying, and Jure Leskovec. 2017. Inductive representation learning on large graphs. In *Proceedings of the 31st International Conference on Neural Information Processing Systems*, pages 1025–1035.
- Devamanyu Hazarika, Roger Zimmermann, and Soujanya Poria. 2020. Misa: Modality-invariant and-specific representations for multimodal sentiment analysis. In *Proceedings of the 28th ACM International Conference on Multimedia*, pages 1122–1131.
- Nancy Helm-Estabrooks. 2002. Cognition and aphasia: a discussion and a study. *Journal of communication disorders*, 35(2):171–186.
- Fabiane Hirsch Kruse. 2013. [Aphasiabank english protocol pwa tucson corpus](#).
- Elizabeth Hoover. 2013. [Aphasiabank english protocol pwa bu corpus](#).
- Judy Illes. 1989. Neurolinguistic features of spontaneous language production dissociate three forms of neurodegenerative disease: Alzheimer’s, huntington’s, and parkinson’s. *Brain and language*, 37(4):628–642.
- Susan Jackson. 2013. [Aphasiabank english protocol pwa kansas corpus](#).
- Daniel Kempler. 2013. [Aphasiabank english protocol pwa kempler corpus](#).
- Andrew Kertesz. 2007. Western aphasia battery–revised.
- Jacquie Kurland. 2013. [Aphasiabank english protocol pwa kurland corpus](#).
- Lucette Lanyon and Miranda L Rose. 2009. Do the hands have it? the facilitation effects of arm and hand gesture on word retrieval in aphasia. *Aphasiology*, 23(7-8):809–822.
- Duc Le, Keli Licata, and Emily Mower Provost. 2018. Automatic quantitative analysis of spontaneous aphasic speech. *Speech Communication*, 100:1–12.
- Duc Le and Emily Mower Provost. 2016. Improving automatic recognition of aphasic speech with aphasiabank. In *Interspeech*, pages 2681–2685.
- Zijie Lin, Bin Liang, Yunfei Long, Yixue Dang, Min Yang, Min Zhang, and Ruifeng Xu. 2022. [Modeling intra- and inter-modal relations: Hierarchical graph contrastive learning for multimodal sentiment analysis](#). In *Proceedings of the 29th International Conference on Computational Linguistics*, pages 7124–7135, Gyeongju, Republic of Korea. International Committee on Computational Linguistics.
- Yinhan Liu, Myle Ott, Naman Goyal, Jingfei Du, Mandar Joshi, Danqi Chen, Omer Levy, Mike Lewis, Luke Zettlemoyer, and Veselin Stoyanov. 2019. Roberta: A robustly optimized bert pretraining approach. *arXiv preprint arXiv:1907.11692*.
- Ilya Loshchilov and Frank Hutter. 2017. Decoupled weight decay regularization. *arXiv preprint arXiv:1711.05101*.
- Jérôme Louradour. 2023. whisper-timestamped. <https://github.com/linto-ai/whisper-timestamped>.
- Camillo Lugaresi, Jiuqiang Tang, Hadon Nash, Chris McClanahan, Esha Uboweja, Michael Hays, Fan Zhang, Chuo-Ling Chang, Ming Guang Yong, Juhyun Lee, et al. 2019. Mediapipe: A framework for building perception pipelines. *arXiv preprint arXiv:1906.08172*.
- Brian MacWhinney. 2013. [Aphasiabank english protocol pwa cmu corpus](#).
- Brian MacWhinney, Davida Fromm, Margaret Forbes, and Audrey Holland. 2011. Aphasiabank: Methods for studying discourse. *Aphasiology*, 25(11):1286–1307.
- Denise McCall. 2013. [Aphasiabank english protocol pwa scale corpus](#).

- Namita Multani, Sebastiano Galantucci, Stephen M Wilson, Tal Shany-Ur, Pardis Poorzand, Matthew E Growdon, Jung Yun Jang, Joel H Kramer, Bruce L Miller, Katherine P Rankin, et al. 2017. Emotion detection deficits and changes in personality traits linked to loss of white matter integrity in primary progressive aphasia. *NeuroImage: Clinical*, 16:447–454.
- Maria Muñoz. 2013. [Aphasiabank english protocol pwa tcu corpus](#).
- Sabiha Parveen and Siva Priya Santhanam. 2021. Speech-language pathologists’ perceived competence in working with culturally and linguistically diverse clients in the united states. *Communication Disorders Quarterly*, 42(3):166–176.
- Xiangdong Pei, Ke Zuo, Yuan Li, and Zhengbin Pang. 2023. A review of the application of multi-modal deep learning in medicine: Bibliometrics and future directions. *International Journal of Computational Intelligence Systems*, 16(1):1–20.
- Basil C Preisig, Noëmi Eggenberger, Dario Cazzoli, Thomas Nyffeler, Klemens Gutbrod, Jean-Marie Annoni, Jurka R Meichtry, Tobias Nef, and René M Müri. 2018. Multimodal communication in aphasia: Perception and production of co-speech gestures during face-to-face conversation. *Frontiers in human neuroscience*, 12:200.
- Ying Qin, Tan Lee, Siyuan Feng, and Anthony Pak-Hin Kong. 2018a. Automatic speech assessment for people with aphasia using tdnn-blstm with multi-task learning. In *Interspeech*, pages 3418–3422.
- Ying Qin, Tan Lee, and Anthony Pak Hin Kong. 2018b. Automatic speech assessment for aphasic patients based on syllable-level embedding and suprasegmental duration features. In *2018 IEEE International Conference on Acoustics, Speech and Signal Processing (ICASSP)*, pages 5994–5998. IEEE.
- Ying Qin, Tan Lee, and Anthony Pak Hin Kong. 2019a. Automatic assessment of speech impairment in cantonese-speaking people with aphasia. *IEEE journal of selected topics in signal processing*, 14(2):331–345.
- Ying Qin, Tan Lee, and Anthony Pak Hin Kong. 2019b. Combining phone posteriorgrams from strong and weak recognizers for automatic speech assessment of people with aphasia. In *ICASSP 2019-2019 IEEE International Conference on Acoustics, Speech and Signal Processing (ICASSP)*, pages 6420–6424. IEEE.
- Alec Radford, Jong Wook Kim, Tao Xu, Greg Brockman, Christine McLeavey, and Ilya Sutskever. 2022. Robust speech recognition via large-scale weak supervision. *arXiv preprint arXiv:2212.04356*.
- Wasifur Rahman, Md Kamrul Hasan, Sangwu Lee, AmirAli Bagher Zadeh, Chengfeng Mao, Louis-Philippe Morency, and Ehsan Hoque. 2020a. [Integrating multimodal information in large pretrained transformers](#). In *Proceedings of the 58th Annual Meeting of the Association for Computational Linguistics*, pages 2359–2369, Online. Association for Computational Linguistics.
- Wasifur Rahman, Md Kamrul Hasan, Sangwu Lee, AmirAli Bagher Zadeh, Chengfeng Mao, Louis-Philippe Morency, and Ehsan Hoque. 2020b. [Integrating multimodal information in large pretrained transformers](#). In *Proceedings of the 58th Annual Meeting of the Association for Computational Linguistics*, pages 2359–2369, Online. Association for Computational Linguistics.
- Amy Ramage. 2013. [Aphasiabank english protocol pwa unh corpus](#).
- General Data Protection Regulation. 2018. General data protection regulation (gdpr). *Intersoft Consulting*, Accessed in October, 24(1).
- Janet Richardson. 2008. [Aphasiabank english controls richardson corpus](#).
- Morteza Rohanian, Julian Hough, and Matthew Purver. 2021. [Alzheimer’s Dementia Recognition Using Acoustic, Lexical, Disfluency and Speech Pause Features Robust to Noisy Inputs](#). In *Proc. Interspeech 2021*, pages 3820–3824.
- Saryu Sharma, Patrick M Briley, Heather Harris Wright, Jamie L Perry, Xiangming Fang, and Charles Ellis. 2019. Gender differences in aphasia outcomes: Evidence from the aphasiabank. *International Journal of Language & Communication Disorders*, 54(5):806–813.
- Maura Silverman. 2013. [Aphasiabank english protocol pwa tap corpus](#).
- Brielle Stark. 2022. [Aphasiabank english cc stark corpus](#).
- Brielle Stark. 2023. [Aphasiabank english aphasia neural corpus](#).
- Carol S Swindell, Audrey L Holland, and Davida Fromm. 1984. Classification of aphasia: Wab type versus clinical impression. In *Clinical Aphasiology: Proceedings of the Conference 1984*, pages 48–54. BRK Publishers.
- Muhammad Shehram Shah Syed, Zafi Sherhan Syed, Margaret Lech, and Elena Pirogova. 2020. Automated screening for alzheimer’s dementia through spontaneous speech. *Proc. Interspeech 2020*, pages 2222–2226.
- Gretchen Szabo. 2013. [Aphasiabank english protocol pwa adler corpus](#).
- Pingjie Tang, Meng Jiang, Bryan Ning Xia, Jed W Pitera, Jeffrey Welsler, and Nitesh V Chawla. 2020. Multi-label patent categorization with non-local

- attention-based graph convolutional network. In *Proceedings of the AAAI Conference on Artificial Intelligence*, volume 34, pages 9024–9031.
- Cynthia Thompson. 2013. [Aphasiabank english protocol pwa thompson corpus](#).
- Iván G Torre, Mónica Romero, and Aitor Álvarez. 2021. Improving aphasic speech recognition by using novel semi-supervised learning methods on aphasiabank for english and spanish. *Applied Sciences*, 11(19):8872.
- Yao-Hung Hubert Tsai, Shaojie Bai, Paul Pu Liang, J Zico Kolter, Louis-Philippe Morency, and Ruslan Salakhutdinov. 2019. Multimodal transformer for unaligned multimodal language sequences. In *Proceedings of the 57th Annual Meeting of the Association for Computational Linguistics*, pages 6558–6569.
- Minjie Wang, Da Zheng, Zihao Ye, Quan Gan, Mufei Li, Xiang Song, Jinjing Zhou, Chao Ma, Lingfan Yu, Yu Gai, et al. 2019. Deep graph library: A graph-centric, highly-performant package for graph neural networks. *arXiv preprint arXiv:1909.01315*.
- Mohammad Wasay, Ismail A Khatri, and Subhash Kaul. 2014. Stroke in south asian countries. *Nature reviews neurology*, 10(3):135–143.
- Jochen Weiner, Mathis Engelbart, and Tanja Schultz. 2017. Manual and automatic transcriptions in dementia detection from speech. In *Interspeech*, pages 3117–3121.
- Janet Whiteside. 2013. [Aphasiabank english protocol pwa whiteside corpus](#).
- Darlene Williamson. 2013. [Aphasiabank english protocol pwa williamson corpus](#).
- Stephen Wilson. 2021. [Aphasiabank english protocol pwa aprocsa corpus](#).
- Stephen M Wilson, Dana K Eriksson, Sarah M Schneck, and Jillian M Lucanie. 2018. A quick aphasia battery for efficient, reliable, and multidimensional assessment of language function. *PloS one*, 13(2):e0192773.
- Linda Wozniak. 2013. [Aphasiabank english protocol pwa wozniak corpus](#).
- Heather Wright. 2013. [Aphasiabank english protocol pwa wright corpus](#).
- Jianing Yang, Yongxin Wang, Ruitao Yi, Yuying Zhu, Azaan Rehman, Amir Zadeh, Soujanya Poria, and Louis-Philippe Morency. 2021. Mtag: Modal-temporal attention graph for unaligned human multimodal language sequences. In *Proceedings of the 2021 Conference of the North American Chapter of the Association for Computational Linguistics: Human Language Technologies*, pages 1009–1021.
- Jingfan Yao, Zaizhu Han, Yanli Song, Lei Li, Yun Zhou, Weikang Chen, Yongmei Deng, Yongjun Wang, Yumei Zhang, et al. 2015. Relationship of post-stroke aphasic types with sex, age and stroke types. *World Journal of Neuroscience*, 5(01):34.
- Jeewoo Yoon, Chaewon Kang, Seungbae Kim, and Jinyoung Han. 2022. D-vlog: Multimodal vlog dataset for depression detection. In *Proceedings of the AAAI Conference on Artificial Intelligence*, volume 36, pages 12226–12234.
- Amir Zadeh, Minghai Chen, Soujanya Poria, Erik Cambria, and Louis-Philippe Morency. 2017. Tensor fusion network for multimodal sentiment analysis. *arXiv preprint arXiv:1707.07250*.
- Amir Zadeh, Rowan Zellers, Eli Pincus, and Louis-Philippe Morency. 2016. Multimodal sentiment intensity analysis in videos: Facial gestures and verbal messages. *IEEE Intelligent Systems*, 31(6):82–88.
- Haopeng Zhang, Xiao Liu, and Jiawei Zhang. 2022. [HEGEL: Hypergraph transformer for long document summarization](#). In *Proceedings of the 2022 Conference on Empirical Methods in Natural Language Processing*, pages 10167–10176, Abu Dhabi, United Arab Emirates. Association for Computational Linguistics.

## A Dataset

### A.1 AphasiaBank Dataset

As illustrated in Table 6, we sourced our dataset from the AphasiaBank (MacWhinney et al., 2011; Forbes et al., 2012), a shared multimedia database used by clinicians for aphasia research<sup>5</sup>.

Table 6: The corpora we used from AphasiaBank

Corpus	Site
ACWT (Bynek, 2013)	Aphasia Center of West Texas
Adler (Szabo, 2013)	Adler Aphasia Center
APROCSA (Wilson, 2021)	Vanderbilt University Medical Center
BU (Hoover, 2013)	Boston University
Capilouto (Capilouto, 2008)	University of Kentucky
CC-Stark (Stark, 2022)	file for CC
CMU (MacWhinney, 2013)	Carnegie Mellon University
Elman (Elman, 2011, 2016)	Aphasia Center of California
Fridriksson (Fridriksson, 2013)	University of South Carolina
Garrett (Garrett, 2013)	Pittsburgh, PA
Kansas (Jackson, 2013)	University of Kansas
Kempler (Kempler, 2013)	Emerson College
Kurland (Kurland, 2013)	University of Massachusetts, Amherst
MSU (Boyle, 2013)	Montclair State University
NEURAL (Stark, 2023)	NEURAL Research Lab, Indiana University
Richardson (Richardson, 2008)	University of New Mexico
SCALE (McCall, 2013)	Snyder Center for Aphasia Life Enhancement
STAR (Corwin, 2013)	Stroke Aphasia Recovery Program
TAP (Silverman, 2013)	Triangle Aphasia Project
TCU (Muñoz, 2013)	Texas Christian University
Thompson (Thompson, 2013)	Northwestern University
Tucson (Hirsch Kruse, 2013)	University of Arizona
UCL (Dean, 2021)	University College London
UMD (Faroqi-Shah and Milman, 2018)	University of Maryland
UNH (Ramage, 2013)	University of New Hampshire
Whiteside (Whiteside, 2013)	University of Central Florida
Williamson (Williamson, 2013)	Stroke Comeback Center
Wozniak (Wozniak, 2013)	InteRACT
Wright (Wright, 2013)	Arizona State University

Table 7: Comparison of the number of samples in 50 Token data and 30 Token data.

Labels	Impaired		Aphasia Types	# Sample	
	Flu.	Com.		50 tokens (ours)	30 tokens
Ctrl.	✗	✗	Control	1,815	3,157
Flu.	✗	✗	Anomic	927	1,639
			Conduction	424	753
Non-Com.	✗	✓	Trans. Sensory	3	5
			Wernicke	188	331
Non-Flu.	✓	✗	Trans. Motor	23	44
			Broca	271	518
Total				3,651	6,447

Table 8: The Word Error Rate (WER) across Aphasia Types for all participants.

Labels	Impaired		Aphasia Types	Average WER	
	Flu.	Com.		Raw	Pre-proc.
Ctrl.	✗	✗	Control	0.332	0.18
Flu.	✗	✗	Anomic	0.714	0.623
			Conduction		
Non-Com.	✗	✓	Trans. Sensory Wernicke	0.607	0.542
Non-Flu.	✓	✗	Trans. Motor Broca	0.967	0.974
Total				0.615	0.521

<sup>5</sup><https://talkbank.org/share/citation.html>

### A.2 Aphasia Types

As shown in Figure 5 in Appendix, aphasia can be classified into eight types based on the Western Aphasia Battery (WAB) (Kertesz, 2007), a standard protocol for categorizing patients based on the most prominent symptoms and severity, and they are next broken down by the ability to auditory comprehension and fluency skills.

### A.3 Disfluency Keywords

Table 9 shows the examples of disfluency keywords  $f$ .

Table 9: The examples of disfluency keywords  $f$

Disfluency Tokens
'[*]', 'the', 'and', 'to', 'um', 'she', 'a', 'her', 'was', 'they', 'so', 'that', 'of', 'cinderella', 'it', 'uh', 'in', 'i', 'he', 'but', 'all', 'is', 'had', 'then', 'ball', 'go', 'with', 'prince', 'this', 'one', 'on', 'you', 'two', 'there', 'were', 'for', 'going', 'king', 'be', 'know', 'out', 'at', 'no', 'not', 'like', 'slipper', 'get', 'have', 'dress', 'got', 'up', 'went', 'very', 'who', 'glass', 'because', 'or', 'time', 'oh', 'stepmother', 'into', 'do', 'shes', 'what', 'beautiful', 'back', 'its', 'home', 'girl', 'woman', 'fairy', 'when', 'godmother', 'would', 'said', 'just', 'as', 'has', 'little', 'shoe', 'well', 'dont', 'his', 'mother', 'them', 'daughters', 'house', 'midnight', 'stepsisters', 'by', 'men', 'bye', 'girls', 'sisters', 'mice', 'everything', 'fit', 'came', 'other', 'goes'

### A.4 Analysis on Gesture Difference

We applied ANOVA to assess the differences in gesture features among the different aphasia types groups as well as the control group, as shown in Table 11. This analysis allowed us to determine whether there are significant differences in gesture patterns between the aphasia types.

## B Experiment

### B.1 Experimental Settings

As shown in Table 10, we split the dataset into the train and test sets with a 8:2 ratio. We tune hyperparameters based on the highest F1 score obtained from the cross-validation set for the models. We use the grid search to explore the dimension of hidden state  $U_i \in \{64, 128, 256, 512, 768\}$ , number of LSTM layers  $n \in \{1, 2, 5\}$ , dropout  $\sigma \in \{0.1, 0.2, 0.3, 0.4, 0.5\}$ , and initial learning rate  $lr \in \{1e-5, 2e-5, 3e-5, 5e-5\}$ . The optimal hyperparameters were found to be:  $U_i = 768$ ,

Table 10: Gender distribution in the dataset.

Gender	Train	Test	Total
All	2,947	704	3,651
Female	1,633	327	1,960
Male	1,314	377	1,691

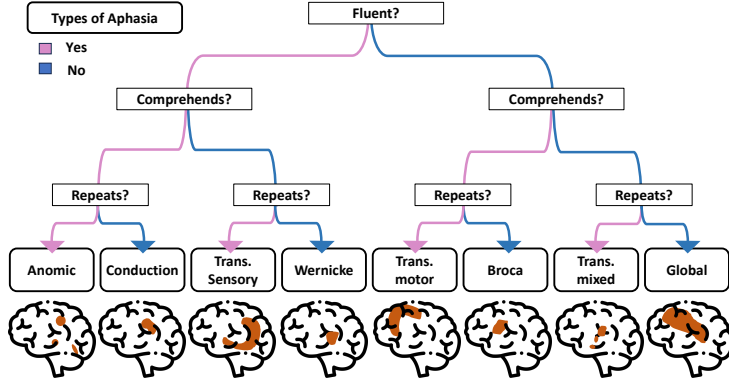


Figure 5: Types of Aphasia

Table 11: Comparison of gesture characteristics among different groups based on Aphasia types using ANOVA. The table below presents the p-values from comparing the gesture features of the top 10 tokens with the highest occurrence. (\*\* means p-value < 0.001 / \* means p-value < 0.05)

Keypoints	[*]	the	and	to	um	she	a	her	was	they
NOSE	0.000 **	0.000 **	0.000 **	0.0099 *	0.000 **	0.000 **	0.000 **	0.000 **	0.000 **	0.2223
LEFT_EYE_INNER	0.000 **	0.000 **	0.000 **	0.0202 *	0.000 **	0.000 **	0.000 **	0.000 **	0.000 **	0.3069
LEFT_EYE	0.000 **	0.000 **	0.000 **	0.000 **	0.016 *	0.000 **	0.000 **	0.000 **	0.000 **	0.2201
LEFT_EYE_OUTER	0.000 **	0.000 **	0.000 **	0.000 **	0.0397 *	0.000 **	0.000 **	0.000 **	0.000 **	0.1535
RIGHT_EYE_INNER	0.2061	0.000 **	0.0858	0.3253	0.000 **	0.1162	0.0143 *	0.000 **	0.000 **	0.4163
RIGHT_EYE	0.000 **	0.000 **	0.0137 *	0.2313	0.000 **	0.1287	0.0094 *	0.000 **	0.000 **	0.243
LEFT_EYE_OUTER	0.000 **	0.000 **	0.000 **	0.0498 *	0.000 **	0.0518	0.000 **	0.000 **	0.000 **	0.0819
LEFT_EAR	0.000 **	0.000 **	0.0614	0.7237	0.0562	0.0481 *	0.6547	0.000 **	0.000 **	0.9854
RIGHT_EAR	0.000 **	0.000 **	0.000 **	0.000 **	0.000 **	0.000 **	0.000 **	0.000 **	0.000 **	0.000 **
MOUTH_LEFT	0.000 **	0.000 **	0.000 **	0.000 **	0.0057 *	0.000 **	0.000 **	0.000 **	0.000 **	0.1522
MOUTH_RIGHT	0.1881	0.000 **	0.0958	0.2863	0.000 **	0.163	0.0185 *	0.000 **	0.000 **	0.4538
LEFT_SHOULDER	0.000 **	0.000 **	0.000 **	0.000 **	0.3065	0.000 **	0.000 **	0.000 **	0.000 **	0.2222
RIGHT_SHOULDER	0.000 **	0.000 **	0.000 **	0.000 **	0.000 **	0.000 **	0.000 **	0.000 **	0.000 **	0.000 **
LEFT_ELBOW	0.000 **	0.000 **	0.000 **	0.000 **	0.6054	0.000 **	0.000 **	0.000 **	0.000 **	0.000 **
RIGHT_ELBOW	0.000 **	0.000 **	0.000 **	0.000 **	0.000 **	0.000 **	0.000 **	0.000 **	0.000 **	0.000 **
LEFT_WRIST	0.000 **	0.000 **	0.000 **	0.000 **	0.2786	0.000 **	0.000 **	0.000 **	0.000 **	0.000 **
RIGHT_WRIST	0.000 **	0.000 **	0.000 **	0.000 **	0.000 **	0.000 **	0.000 **	0.000 **	0.000 **	0.000 **
LEFT_PINKY	0.000 **	0.000 **	0.000 **	0.000 **	0.7116	0.000 **	0.000 **	0.000 **	0.000 **	0.000 **
RIGHT_PINKY	0.000 **	0.000 **	0.000 **	0.000 **	0.000 **	0.000 **	0.000 **	0.000 **	0.000 **	0.000 **
LEFT_INDEX	0.000 **	0.000 **	0.000 **	0.000 **	0.6041	0.000 **	0.000 **	0.000 **	0.000 **	0.000 **
RIGHT_INDEX	0.000 **	0.000 **	0.000 **	0.000 **	0.000 **	0.000 **	0.000 **	0.000 **	0.000 **	0.000 **
LEFT_THUMB	0.000 **	0.000 **	0.000 **	0.000 **	0.4492	0.000 **	0.000 **	0.000 **	0.000 **	0.000 **
RIGHT_THUMB	0.000 **	0.000 **	0.000 **	0.000 **	0.000 **	0.000 **	0.000 **	0.000 **	0.000 **	0.000 **

$n = 2$ ,  $\sigma = 0.1$ , and  $lr = 1e - 5$ . We implement all the methods using PyTorch 1.12 and optimize with the mini-batch AdamW (Loshchilov and Hutter, 2017) with a batch size of 32. We use the Exponential Learning rate Scheduler with gamma 0.001. We train the model on a GeForce RTX 3090 GPU for 50 epochs and apply early stopping with patience of 7 epochs.

## B.2 Baselines

**Aphasia & Dementia Detection Baselines.** Aphasia and dementia are neurological disorders that affect language and cognition, leading to difficulties in various cognitive functions and communication. Aphasia is caused by specific brain damage, resulting in language impairments, while dementia

involves brain neuron degeneration, leading to overall cognitive decline and possible language impairments. Although both disorders impact language and cognition, a clear understanding of their differences and similarities is required for individual diagnosis and assessment.

- **LR** (Cui et al., 2021; Syed et al., 2020): We employed a Logistic Regression Classifier with an added L2 penalty term, using a cost parameter  $c$  value of 0.01.
- **SVM+Poly** (Qin et al., 2018b; Rohanian et al., 2021): Each subject’s text and audio embedding vector is fed to a Support Vector Machine with a polynomial kernel using the cost parameter  $c = 0.01$ .

Table 12: Performance comparisons of the proposed model and baselines including precision, recall and F1-score.

Model		Ctrl. (355)			Flu. (269)			No-Com. (31)			No-Flu. (49)			Weighted avg. (704)		
		Prec	Rec.	F1	Prec	Rec.	F1	Prec	Rec.	F1	Prec	Rec.	F1	Prec	Rec.	F1
Aphasia & Other Disorder Detection	SVM + Poly	0.504	1.000	0.670	0.000	0.000	0.000	0.000	0.000	0.000	0.000	0.000	0.000	0.254	0.504	0.338
	RF	0.848	0.896	0.871	0.693	0.747	0.719	0.000	0.000	0.000	0.516	0.327	0.400	0.728	0.760	0.742
	DT	0.831	0.817	0.824	0.660	0.643	0.652	0.083	0.097	0.090	0.263	0.306	0.283	0.693	0.683	0.688
	LR	0.779	0.766	0.773	0.611	0.807	0.696	0.000	0.000	0.000	0.000	0.000	0.000	0.627	0.695	0.655
	AdaBoost	0.928	0.839	0.882	0.629	0.699	0.662	0.000	0.000	0.000	0.257	0.367	0.303	0.726	0.716	0.719
Multimodal	MISA	0.846	0.960	0.899	0.725	0.758	0.741	0.000	0.000	0.000	0.785	0.224	0.349	0.758	0.789	0.761
	MuT	0.885	0.885	0.885	0.699	0.810	0.750	0.000	0.000	0.000	0.552	0.327	0.410	0.751	0.778	0.761
	MAG	0.914	0.775	0.838	0.625	0.792	0.698	0.000	0.000	0.000	0.482	0.551	0.514	0.733	0.732	0.725
	SP-Trans.	0.867	0.921	0.893	0.695	0.796	0.742	0.000	0.000	0.000	0.579	0.224	0.324	0.743	0.784	0.756
<b>Ours</b>		0.949	0.949	0.949	0.799	0.885	0.840	0.176	0.097	0.125	0.647	0.449	0.530	0.837	0.852	0.842

- **Random Forest** (Cui et al., 2021; Balagopalan et al., 2020): The Random Forest classifier has demonstrated improved performance in various speech classification tasks, including speech/non-speech discrimination and speech emotion recognition.
- **Decision Tree** (Qin et al., 2018b; Balagopalan and Novikova, 2021): For the decision tree model, the text and audio embedding vectors of each subject are used as input. The model is trained using the gini criterion.
- **AdaBoost** (Cui et al., 2021): We set the maximum number of estimators to 50 and apply the boosting algorithm for AdaBoost.

**Multimodal fusion Baselines.** To accurately classify types of aphasia, we use multimodal data consisting of text, video, and audio. Our aim is to demonstrate the effectiveness of our model compared to existing multimodal sentiment analysis baseline models, highlighting its validity in the context of aphasia.

- **MuT** (Tsai et al., 2019): The MuT model is designed for analyzing multimodal human language. It utilizes a crossmodal attention mechanism to fuse multimodal information by directly attending to low-level features in other modalities.
- **MISA** (Hazari et al., 2020): MISA operates two subspaces for each modality: a modality-invariant subspace that captures commonalities and reduces modality gaps, and a modality-specific subspace that captures distinctive features. These representations enable a holistic view of multimodal data, which is used for fusion and task predictions.
- **MAG** (Rahman et al., 2020b): MAG is a method introduced for efficient finetuning of large pre-

trained Transformer models for multimodal language processing. It represents nonverbal behavior as a vector with trajectory and magnitude, allowing it to shift lexical representations within the pre-trained Transformer model.

- **SP-Transformer** (Cheng et al., 2021): SP-Transformer uses a sampling function to create a sparse attention matrix, reducing long sequences to shorter hidden states. The model captures interactions between hidden states of different modalities at each layer. To improve efficiency, it employs Layer-wise parameter sharing and Factorized Co-Attention, minimizing the impact on task performance.

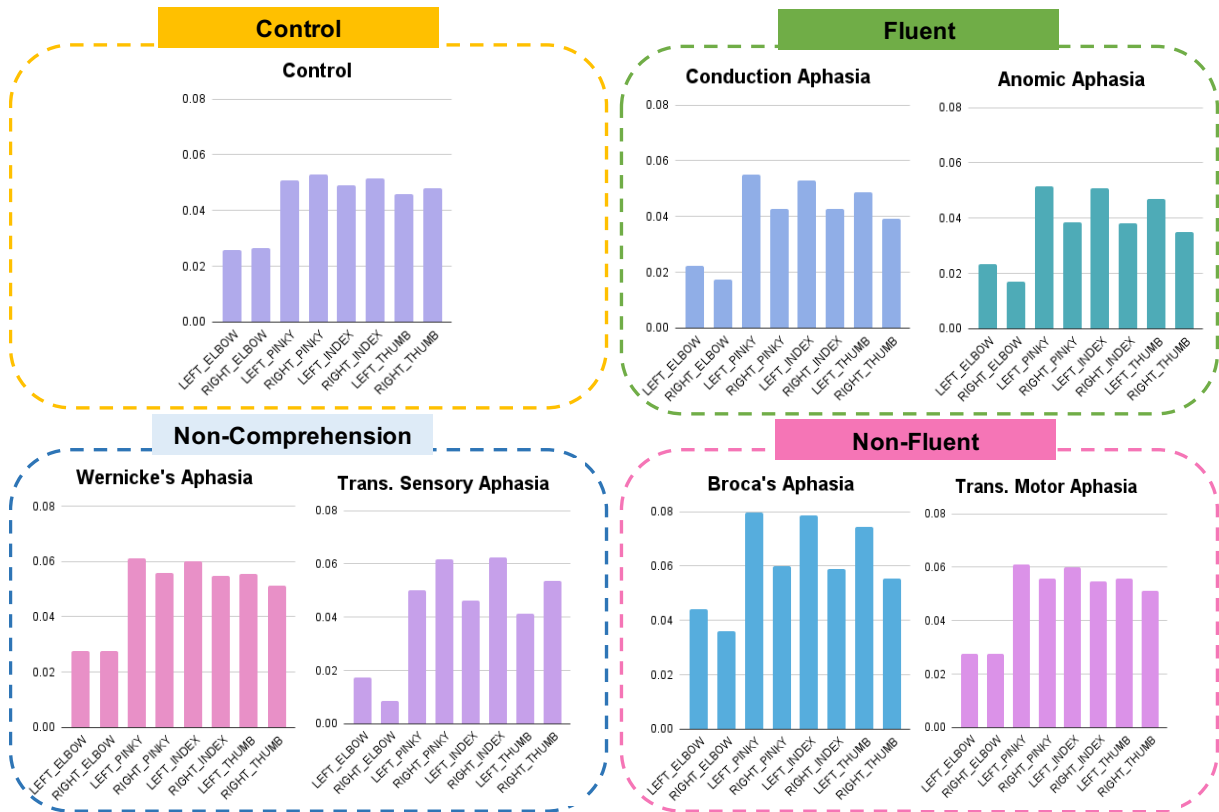


Figure 6: Visualization of the standard deviation values for pose key points of each aphasia type

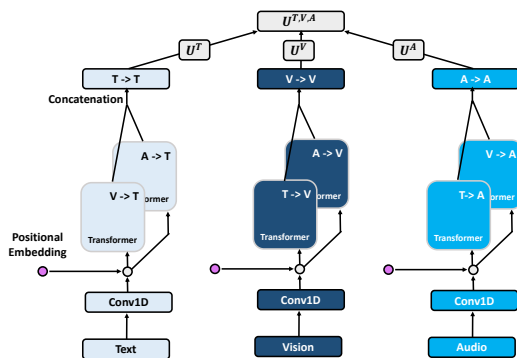


Figure 7: Architecture of Multimodal Transformer Encoder (Rahman et al., 2020b)